

## V<sub>2</sub>O<sub>3</sub>(0001) Surface Termination: Phase Equilibrium

A. J. Window,<sup>1</sup> A. Hentz,<sup>1,\*</sup> D. C. Sheppard,<sup>1</sup> G. S. Parkinson,<sup>1,†</sup> H. Niehus,<sup>2,‡</sup> D. Ahlbehrendt,<sup>2</sup> T. C. Q. Noakes,<sup>3</sup> P. Bailey,<sup>3</sup> and D. P. Woodruff<sup>1,4,§</sup>

<sup>1</sup>Physics Department, University of Warwick, Coventry CV4 7AL, United Kingdom

<sup>2</sup>Humboldt-Universität zu Berlin, Institut für Physik, Newtonstrasse. 15, D-12489 Berlin, Germany

<sup>3</sup>STFC Daresbury Laboratory, Warrington WA4 4AD, United Kingdom

<sup>4</sup>Fritz-Haber-Institut der Max-Planck-Gesellschaft, Faradyweg 4-6, 14195 Berlin, Germany

(Received 29 March 2011; published 1 July 2011)

Complementary but independent medium-energy and low-energy ion scattering studies of the (0001) surfaces of V<sub>2</sub>O<sub>3</sub> films grown on Pd(111), Au(111) and Cu<sub>3</sub>Au(100) reveal a reconstructed full O<sub>3</sub>-layer termination creating a VO<sub>2</sub> surface trilayer. This structure is fully consistent with previous calculations based on thermodynamic equilibrium at the surface during growth, but contrasts with previous suggestions that the surface termination comprises a complete monolayer of vanadyl (V = O) species.

DOI: 10.1103/PhysRevLett.107.016105

PACS numbers: 68.35.B-, 68.47.Gh, 68.49.Sf

Oxide surfaces, and particularly those of vanadium oxides, play a major role in heterogeneous catalysis [1], yet there have been very few quantitative experimental structure determinations. The (0001) faces of the corundum-phase structures V<sub>2</sub>O<sub>3</sub>, α-Al<sub>2</sub>O<sub>3</sub>, and Cr<sub>2</sub>O<sub>3</sub>, are particularly interesting because there are several distinctly different atomic layers at which the bulk structure might be terminated. One fundamental question is whether, in practice, these surfaces can be created in a state that is truly in equilibrium with their surroundings under preparation conditions. Starting from a bulk crystal one might anticipate difficulty in overcoming the kinetic barriers to achieve this equilibrium under conditions of temperature and oxygen partial pressure accessible to surface science experiments. Alternatively, epitaxial growth of the oxide on a suitable substrate, by deposition of metal vapor in the presence of a partial pressure of oxygen, may offer a better means of achieving this gas-solid equilibrium. Growth is intrinsically a nonequilibrium process, yet using low metal deposition rates in an excess of oxygen gas, the kinetic barriers to achieving equilibrium may be much lower than those needed to modify an existing nonequilibrium surface. In fact, previous structural studies of the surface of bulk crystals of α-Al<sub>2</sub>O<sub>3</sub> and Cr<sub>2</sub>O<sub>3</sub>, and of Cr<sub>2</sub>O<sub>3</sub> produced by oxidation of metallic Cr, appear to be broadly consistent with the theoretically predicted equilibrium structure. By contrast, spectroscopic, imaging, and chemical studies of the V<sub>2</sub>O<sub>3</sub>(0001) surface of epitaxial films grown *in situ* have been interpreted in terms of a nonequilibrium surface (e.g., [2–6]). Here we show that two independent quantitative experimental determinations of the structure of V<sub>2</sub>O<sub>3</sub>(0001), using distinctly different ion scattering methods, demonstrate that the structure *does* correspond to the equilibrium state predicted in density functional theory (DFT) calculations. We find this is true for the surfaces of films grown under conditions that are both similar to, and distinctly different from, those used in the earlier

explorations of these surfaces. We discuss how these apparently conflicting views may be reconciled.

Relative to the (0001) basal plane, the bulk structure of V<sub>2</sub>O<sub>3</sub> comprises alternate buckled layers containing 2 metal atoms per unit mesh, and planar layers containing 3 oxygen atoms per unit mesh; this layer structure is denoted here as ...O<sub>3</sub>VV'O<sub>3</sub>VV'O<sub>3</sub>VV'... (Fig. 1). Three distinct stoichiometric terminations of this bulk structure can be envisaged, namely, oxygen ...VV'O<sub>3</sub>, full-metal ...O<sub>3</sub>VV', (both polar surfaces), and half-metal ...V'O<sub>3</sub>V. Vibrational spectroscopy [2,3] indicates that vanadyl species, V = O, occur on the surface, and this, together with scanning tunneling microscopy images [4] and x-ray absorption spectroscopy [5], has been interpreted as indicating that the stable structure is half-metal terminated but with O atoms atop all surface V atoms to produce a (1 × 1) vanadyl phase (Fig. 1). However, DFT calculations show [7,8] that for typical preparation temperatures (~600–900 K), and partial pressure of oxygen (~10<sup>-7</sup>–10<sup>-5</sup> mbar), the equilibrium surface structure should actually be oxygen terminated, possibly with partial coverage of V = O species on this surface (Fig. 2). This O<sub>3</sub> termination is found to be stabilized by a reconstruction in which the upper half-layer of V atoms in the

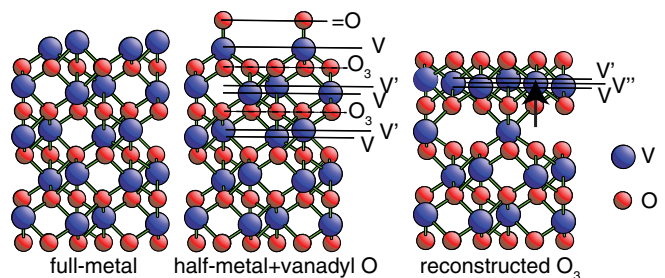


FIG. 1 (color online). Side views (viewed along  $[2\bar{1}10]$ ) of V<sub>2</sub>O<sub>3</sub>(0001), showing three possible surface terminations. In the reconstructed O<sub>3</sub> termination second-layer V' atoms move up to become V'' atoms in the outermost metal layer (see arrow).

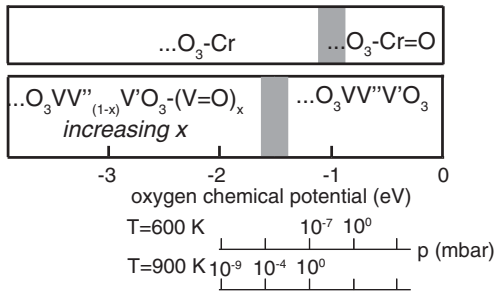


FIG. 2. Simplified diagram showing the equilibrium surface phases of the  $V_2O_3(0001)$  and  $Cr_2O_3(0001)$  surfaces under different conditions of oxygen partial pressure and temperature in DFT calculations [7,25]. For  $V_2O_3$  the region on the left corresponds to partial coverage of vanadyl  $V=O$  species; the calculations considered only two specific values of  $x$ , with  $x = 1/3$  corresponding to the chemical potential range  $\sim -2.7$  to  $-1.5$  eV, and  $x = 2/3$  for larger (negative) values. The diffuse phase boundaries reflect some uncertainty in the associated chemical potential values, as reflected, for example, by different calculations for  $V_2O_3$  [7,8].

second  $VV'$  layer move up into the outermost  $VV'$  layer to produce a  $\dots VO_3VV''V'O_3$  structure. The outermost  $O_3V_3O_3$  layers then have the stoichiometry and local structure characteristic of  $VO_2$ . According to these DFT results, the  $(1 \times 1)$  pure vanadyl termination,  $\dots V'O_3V=O$ , is never the equilibrium structure, but is closest to equilibrium at oxygen chemical potential values beyond the left-hand edge of Fig. 2, far from those achievable experimentally. The only previously published experimental structural study, using photoelectron diffraction, indicated a half-metal termination, with or without vanadyl O atoms, but did not consider the possibility of the  $O_3$  termination [9]. An unpublished low-energy electron diffraction (LEED) study has found good theory-experiment agreement for the vanadyl-terminated structure [10].

The studies reported here used the techniques of medium-energy ion scattering (MEIS) and low-energy noble gas impact-collision ion scattering spectroscopy with detection of neutrals (NICISS) using, respectively, 100 keV  $H^+$  and 3 keV  $He^+$  incident ions. MEIS experiments were performed at the Daresbury Laboratory UK National MEIS facility [11] on  $V_2O_3(0001)$  films grown *in situ* on Pd(111) and Au(111) substrates. NICISS data, obtained in a true  $180^\circ$  backscattering geometry [12], were obtained at the Humboldt University in Berlin [13] on  $V_2O_3(0001)$  films grown on a  $Cu_3Au(100)$  substrate. Note that the symmetries of the substrates contain elements not present in  $V_2O_3$  [mirror planes on fcc(111) surface, mirror planes and fourfold rotation on fcc(100)] leading to multiple mirror and rotational domains with equal occupation in the oxide films. On Pd(111), films  $\sim 20$  Å thickness were grown using a sequence of  $\sim 5$  doses of  $\sim 10$  mins V vapor deposition in  $2 \times 10^{-7}$  mbar of oxygen at a sample temperature of  $\sim 570$  K, followed by heating to  $\sim 670$  K

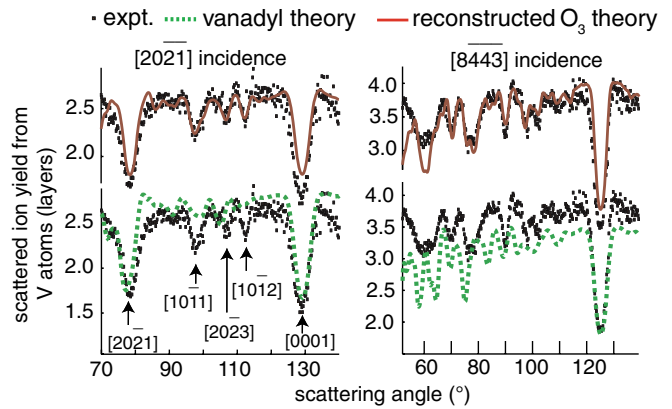


FIG. 3 (color online). Comparison of experimental 100 keV  $H^+$  MEIS blocking curves from  $V_2O_3(0001)$  grown on Au(111), recorded in two different incidence directions, with the results of VEGAS simulations for the reconstructed  $O_3$  and vanadyl termination models. The scattered ion yield is expressed in terms of the number of contributing atomic layers.

for 1–2 mins in vacuum. On Au(111), films up to 200 Å thickness were grown using a single dose (1–3 hours) at the same temperature and oxygen pressure, followed by annealing for 10–20 mins at 770 K in  $5 \times 10^{-8}$  mbar of oxygen. Both methods are closely similar to those used previously by others [3,4]. Growth on  $Cu_3Au(100)$ , oxygen pretreated to form a CAOS (Copper Au Oxygen surface) substrate, involved depositing V at 300 K, followed by annealing at 650 K in  $5 \times 10^{-7}$  mbar oxygen, leading to a  $V_2O_3(0001)$  film thickness of  $\sim 25$  Å [13,14].

Both ion scattering methods exploit the “shadow cones” created by elastic scattering from surface atoms, which exclude ions from regions behind the scattering atoms. In MEIS [15] (shadow cone width  $\sim 0.2$ – $0.3$  Å), specific incident geometries are chosen to illuminate a few near-surface atomic layers, and one exploits the shadow cones produced by the scattering from near-surface atoms that “block” the outward trajectories of ions first scattered by atoms from lower atomic layers. Dips in the “blocking curve” of scattered ion intensity as a function of scattering angle are thus characteristic of the relative positions of atoms in the outermost few atomic layers. In NICISS [12], using much lower energies, and  $He^+$  rather than  $H^+$  incident ions, the much stronger scattering and resulting wider shadow cones ( $\sim 2$  Å) preclude significant subsurface scattering. Using a  $180^\circ$  scattering angle ensures that shadowing effects are almost identical in incidence and scattered trajectories, so one can exploit the near-neighbor shadowing of the outermost layer atoms using fixed grazing incidence angles and variable azimuthal angles.

Figure 3 shows experimental MEIS blocking curves of scattering from V atoms, recorded at two different crystallographic incidence directions, compared with the results of simulations using the VEGAS computer code [16], for two different structural models. These experimental data

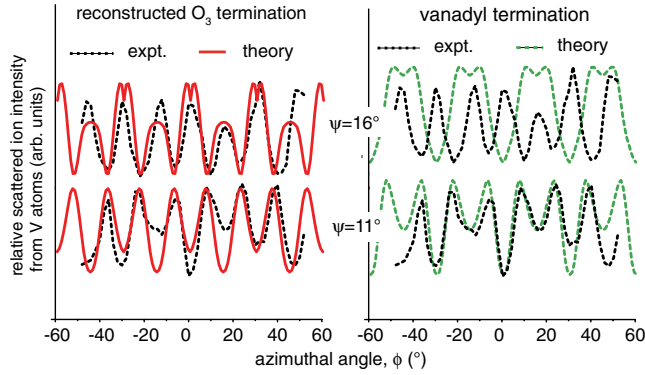


FIG. 4 (color online). Comparison of experimental 3 keV He<sup>+</sup> NICISS azimuthal scans from V<sub>2</sub>O<sub>3</sub>(0001) grown on Cu<sub>3</sub>Au(100), recorded at two different grazing incidence angles, with the results of simulations for the reconstructed O<sub>3</sub>, and the vanadyl termination models (Fig. 1).

were recorded from a 200 Å V<sub>2</sub>O<sub>3</sub> film grown on Au(111); essentially identical data were obtained from the thinner films grown on Pd(111). Figure 3 shows clearly that the simulations based on the vanadyl termination give poor agreement with the experimental data, despite adjustments to the interlayer spacings to optimize the fits. A simple half-metal termination simulation yields very similar blocking curves. By contrast, the simulation for the reconstructed O<sub>3</sub> termination model gives good agreement with experiment.

Figure 4 shows the key results of the NICISS experiments; azimuthal scans of the scattered ion yield from V atoms, recorded at two different grazing incidence angles, are compared with the results of simulations using the FAN computer code [17] for the same two structural models. For these data, too, the simulations based on the reconstructed O<sub>3</sub> termination model provide a greatly superior description of the experimental data. In particular, all the main maxima in the experimental azimuthal plots recorded at 11° incidence switch to main minima when the incidence angle is increased to 16°; this behavior is reproduced for the O<sub>3</sub> termination, but not for the vanadyl model, nor for other models tested including half-metal and full-metal terminations (not shown). Table I provides a comparison of the best-fit values of the outermost interlayer spacings found in the two experimental studies and in the earlier DFT calculations; the agreement is good and the results are consistent.

This structural conclusion for V<sub>2</sub>O<sub>3</sub>(0001) contrasts with that of previous experimental investigations of other corundum-phase surface structures, α-Al<sub>2</sub>O<sub>3</sub>(0001) [18,19] and Cr<sub>2</sub>O<sub>3</sub>(0001) [20–23]. For α-Al<sub>2</sub>O<sub>3</sub>(0001) the half-metal termination is favored by LEED [18] and surface x-ray diffraction (SXRD) [19] studies, as well as DFT studies [24]. For Cr<sub>2</sub>O<sub>3</sub>(0001) the original LEED study also favored a half-metal termination [20], but later work indicated there may be fractional occupation of other

TABLE I. Interlayer spacings in the reconstructed O<sub>3</sub> model as found in the original DFT study [7] and in the MEIS and NICISS studies reported here. The labelling of the layers from the bulk is ... V'(3)-O<sub>3</sub>(3)-V(2)-O<sub>3</sub>(2)-V(top)-V''(top)-V'(top)-O<sub>3</sub>(top). In NICISS ions do not penetrate to the subsurface layers. The precision in the MEIS and NICISS values is  $\sim \pm 0.1$  Å. Dash entries for NICISS reflect the fact that this technique does not penetrate to deeper layers.

Parameter	DFT [7]	MEIS	NICISS
V'(top)-O <sub>3</sub> (top) (Å)	0.86	0.91	0.85
V''(top)-V'(top) (Å)	0.19	0.18	0.05
V(top)-V''(top) (Å)	0.19	0.18	0.05
O <sub>3</sub> (2)-V(top) (Å)	0.99	0.98	-
V(2)-O <sub>3</sub> (2) (Å)	1.44	1.27	-
O <sub>3</sub> (3)-V(2) (Å)	1.06	0.98	-
V'(3)-O <sub>3</sub> (3) (Å)	(0.98)	1.07	-

sites [21–23]. The main conclusions of the DFT calculations [25] for the predicted equilibrium phases of the surfaces of V<sub>2</sub>O<sub>3</sub>(0001) and Cr<sub>2</sub>O<sub>3</sub>(0001) at different oxygen chemical potential values in the gas phase are summarized in Fig. 2. For values in the range  $-1$  eV to  $-1.5$  eV, typical of the preparation conditions, theory predicts for these two surfaces, the O<sub>3</sub> and half-metal terminations, respectively. Interestingly, at slightly smaller negative oxygen chemical potentials (higher oxygen pressures) the chromyl, Cr = O, termination becomes stable on Cr<sub>2</sub>O<sub>3</sub>, consistent with observation of the associated Cr-O stretching mode in vibrational spectroscopy after oxygen exposure [26]. These results are also broadly consistent with the results of a recent detailed SXRD study [23] which finds a chromyl termination at high oxygen pressures, although at lower pressures partial occupation of half-metal and full-metal sites is found. It appears, therefore, that with the exception of these full-metal sites, *all* these surface studies of corundum-phase surfaces are consistent with the predicted thermodynamic equilibrium, whether produced from bulk crystals, oxidation of a metal crystal, or via epitaxial growth *in situ*. Note that Fig. 2 and this discussion relates to the equilibrium between the surface and gas phase; the DFT studies indicate that under most surface preparation conditions VO<sub>2</sub> and CrO<sub>2</sub> bulk phases are more stable than the V<sub>2</sub>O<sub>3</sub> and Cr<sub>2</sub>O<sub>3</sub>, but these calculations take no account of the stabilizing influence of the substrate epitaxy, nor of the energetic barrier to a bulk structural transformation.

It remains to account for previous conclusions that the V<sub>2</sub>O<sub>3</sub>(0001) surface adopts the nonequilibrium (1 × 1) vanadyl termination. The observation of a vanadyl V = O stretching frequency in vibrational spectroscopy is the most significant evidence for this interpretation, but this provides no information on the vanadyl coverage. In fact *partial* coverage of vanadyl species, on an otherwise reconstructed-O<sub>3</sub> termination, is consistent with the



predicted equilibrium structure within a range of oxygen chemical potentials close to those experienced by the growing crystal (Fig. 2). Our results are not incompatible with this possibility, although we find no explicit evidence for their presence; while ion scattering simulations of (random) partial occupation of different sites cannot easily be performed, we estimate (from Figs. 3 and 4) that up to 10%–20% partial occupation of vanadyl sites could be consistent with our data. A predominantly O<sub>3</sub> termination is also consistent with a photoelectron diffraction study of hydroxylated V<sub>2</sub>O<sub>3</sub>(0001) which found that the hydroxylated O atoms occupied (predominantly or exclusively) sites in a complete O<sub>3</sub> layer, and not in surface vanadyl species [27]. STM might be expected to distinguish the vanadyl termination, with one V = O surface species per unit mesh, from the O<sub>3</sub> termination, with three surface O atoms per unit mesh, but theoretical simulations indicate that both terminations should lead to a single atomic-scale protrusion per unit mesh [28]. There seems good reason, therefore, to reassess the interpretation of some of the conclusions of earlier work on this surface insofar as they are based on the assumption that the surface is fully vanadyl terminated. Our results indicate that is not the case, and that contrary to previous suggestions, the V<sub>2</sub>O<sub>3</sub>(0001) surface structure, like that of Cr<sub>2</sub>O<sub>3</sub>(0001) and  $\alpha$ -Al<sub>2</sub>O<sub>3</sub>(0001), does correspond to that predicted in DFT calculations of the thermodynamic equilibrium with the gas phase under preparation conditions. Specifically, V<sub>2</sub>O<sub>3</sub>(0001) has a reconstructed O<sub>3</sub> termination, albeit with partial vanadyl coverage under some conditions.

The authors acknowledge the financial support of the Deutsche Forschungsgemeinschaft through the Sonderforschungsbereich 546 and the Engineering and Physical Sciences Research Council (UK). Veronica Ganduglia-Pirovano is thanked for valuable discussions.

---

\*Present address: Universidade Federal do Rio Grande do Sul, Inst. de Física 91501-970 Porto Alegre, RS, Brazil.

†Present address: Institut für Angewandte Physik, TU Wien, 1040 Wien, Austria.

‡Also at: Divisão de Metrologia de Materiais (DIMAT), INMETRO, CEP 25250-020, Xerém, Duque de Caxias, RJ, Brazil.

§Corresponding author  
d.p.woodruff@warwick.ac.uk

- [1] B. Grzybowska-Świerkosz and F. Trifirò, *Appl. Catal., A* **157**, 1 (1997).
- [2] J. Schoiswohl *et al.*, *Surf. Sci.* **555**, 101 (2004).
- [3] A. -C. Dupuis *et al.*, *Surf. Sci.* **539**, 99 (2003).
- [4] S. Surnev, M. G. Ramsey, and F. P. Netzer, *Prog. Surf. Sci.* **73**, 117 (2003).
- [5] C. Kolczewski *et al.*, *Surf. Sci.* **601**, 5394 (2007).
- [6] D. Göbke *et al.*, *Angew. Chem., Int. Ed.* **48**, 3695 (2009).
- [7] G. Kresse *et al.*, *Surf. Sci.* **555**, 118 (2004).
- [8] T. K. Todorova, M. V. Ganduglia-Pirovano, and J. Sauer, *J. Phys. Chem. B* **109**, 23523 (2005).
- [9] E. A. Kröger *et al.*, *Surf. Sci.* **601**, 3350 (2007).
- [10] Y. Romanyshyn and H. Kühlenbeck, H. -J. Freund (to be published).
- [11] P. Bailey, T. C. Q. Noakes, and D. P. Woodruff, *Surf. Sci.* **426**, 358 (1999).
- [12] H. Niehus, W. Heiland, and E. Taglauer, *Surf. Sci. Rep.* **17**, 213 (1993).
- [13] H. Niehus, R. -P. Blum, and D. Ahlbehrendt, *Surf. Rev. Lett.* **10**, 353 (2003).
- [14] H. Niehus, R. P. Blum, and D. Ahlbehrendt, *Phys. Status Solidi A* **187**, 151 (2001).
- [15] J. F. van der Veen, *Surf. Sci. Rep.* **5**, 199 (1985).
- [16] R. M. Tromp and J. F. van der Veen, *Surf. Sci.* **133**, 159 (1983).
- [17] H. Niehus and R. Spitzl, *Surf. Interface Anal.* **17**, 287 (1991); a free copy of the FAN code can be requested via e-mail to niehus@physik.hu-berlin.de.
- [18] C. F. Walters *et al.*, *Surf. Sci.* **464**, L732 (2000).
- [19] P. Guénard *et al.*, *Surf. Rev. Lett.* **5**, 321 (1998).
- [20] R. Rohr *et al.*, *Surf. Sci.* **372**, L291 (1997); **389**, 391(E) (1997).
- [21] Th. Gloege *et al.*, *Surf. Sci.* **441**, L917 (1999).
- [22] M. Lübke and W. Moritz, *J. Phys. Condens. Matter* **21**, 134010 (2009).
- [23] O. Bikondoa *et al.*, *Phys. Rev. B* **81**, 205439 (2010).
- [24] R. Di Felice and J. E. Northrup, *Phys. Rev. B* **60**, R16287 (1999).
- [25] A. Rohrbach, J. Hafner, and G. Kresse, *Phys. Rev. B* **70**, 125426 (2004).
- [26] B. Dillmann *et al.*, *Faraday Discuss.* **105**, 295 (1996).
- [27] E. A. Kröger *et al.*, *Surf. Sci.* **602**, 1267 (2008).
- [28] S. Surnev *et al.*, *Surf. Sci.* **495**, 91 (2001).